IGARSS 2022 - 2022 IEEE International Geoscience and Remote Sensing Symposium | 978-1-6654-2792-0/22/$31.00 ©2022 IEEE | DOI: 10.1109/IGARSS46834.2022.9884730

RETRIEVING PHYSICAL PROPERTIES OF THE ANTARCTIC FIRN VIA SPACEBORNE MICROWAVE RADIOMETRY

Rahul Kar[1], Mustafa Aksoy[1], and Dua Kaurejo[1]*

[1]Department of Electrical and Computer Engineering, University at Albany – State University of New York, Albany, NY 12222, USA

ABSTRACT

This paper discusses the retrieval of important physical properties of the Antarctic firn via spaceborne microwave radiometry focusing on Concordia and Vostok stations. Previous studies indicated that microwave radiometer measurements are sensitive to important physical properties of the firn from its surface down to deep isothermal ice. Here we demonstrated how brightness temperature differences measured by spaceborne radiometers over different parts of the Antarctic firn are related to changes in physical properties such as density; thus, retrieval of these properties is possible.

Index Terms— radiometry, Antarctic firn, physical properties, remote sensing, Antarctic firn, Concordia, Vostok.

1. INTRODUCTION

We have previously studied how the Global Precipitation Measurement Constellation can be used as a multi-frequency (11 frequency channels at 6.9 GHz, 7.3 GHz, 10.65 GHz, 18.7 GHz, 19.35 GHz, 22.235 GHz, 23.8 GHz, 36.5 GHz, 37 GHz, 89 GHz, and 91.665 GHz) microwave radiometer system to characterize the Antarctic firn in terms of its physical and thermal properties such as firn temperature, density, and grain size [1]. Following that study, intercalibrated brightness temperature measurements of AMSR2 and SSMIS radiometers in the GPM constellation plus the 6.9 GHz and 7.3 GHz brightness temperature measurements of AMSR2 from January 2020 to June 2021 were collected and averaged monthly over two 0.25ºx0.25º degree latitude-longitude grid cells centered around the Concordia (75°05′59″S 123°19′56″E) and Vostok (78°27′52″S 106°50′2″E) stations in Antarctica. Figure 1 depicts the horizontally polarized brightness temperatures versus month over the Concordia and Vostok stations between January 2020 (Month 1) and December 2020 (Month 12) at all above-mentioned GPM frequencies (except 22.235 GHz since only vertically polarized brightness temperature measurements are available at this frequency). A considerable difference between the brightness temperatures in Concordia and Vostok station can be seen where the brightness temperatures over Concordia is higher than those over Vostok. Variations in physical and thermal properties of the firn can be associated with this difference.

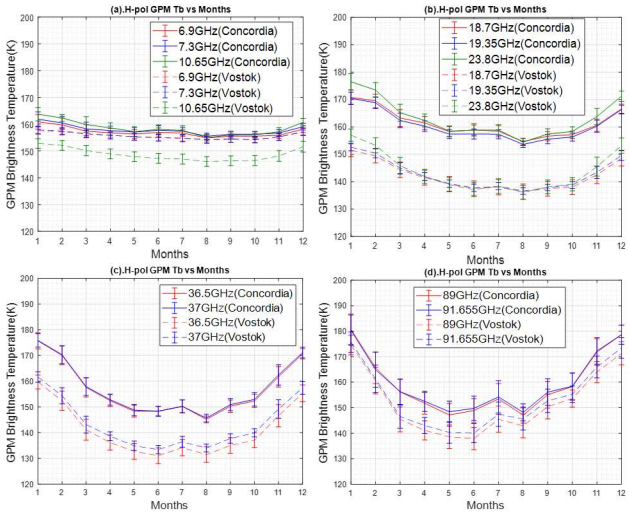

Figure 1: Horizontally polarized brightness temperatures over Concordia and Vostok stations in Antarctica vs months at frequencies (a) 6.9, 7.3 and 10.65 GHz; (b) 18.7, 19.35 and 23.8 GHz; (c) 36.5 and 37 GHz; (d) 89 and 91.655 GHz.

2. PHYSICAL PROPERTIES OF THE FIRN

2.1 Firn Density

Antarctic firn density can be expressed as the sum of an average firn density and finer scale fluctuations due to subsurface layerings as described in [2]:

$$\rho(z) = \rho_\infty - (\rho_\infty - \rho_0)e^{z\beta} + \rho_n(z)e^{z\alpha} \text{ kg/m}^3 \quad (1)$$

where ρ_0 is the near surface density, ρ_∞ is the compacted ice density at depth, $z(<0)$ is depth, and β is a factor that controls densification. $\rho_n(z)$ represents the fluctuations associated with internal layerings which can be modeled as a correlated Gaussian random process described by a standard deviation ($\sigma_{density}$) and a vertical correlation length. These fluctuations are damped with depth according to the damping factor α.

2.2 Grain Radius

In-situ measurements show that the size of ice particles at Concordia is almost double that of Vostok as shown in Figure 2 [3,4]. We defined the grain size profiles in the Antarctic firn based on this in-situ data using linear regression fits. For Concordia and Vostok, the grain radius profiles were modeled as

$$r(z) = \sqrt{(0.5687)^2 + z * (5.074 * 10^{-3})}\ \text{mm} \quad (2)$$

and

$$r(z) = \sqrt{(10^{-3})^2 + z * (9.245 * 10^{-4})}\ \text{mm} \quad (3)$$

respectively where r(z) is the grain size at depth z in meters. However, it is important to note that the fit for Vostok is susceptible to errors due to lack of enough in-situ measurements at shallower depths.

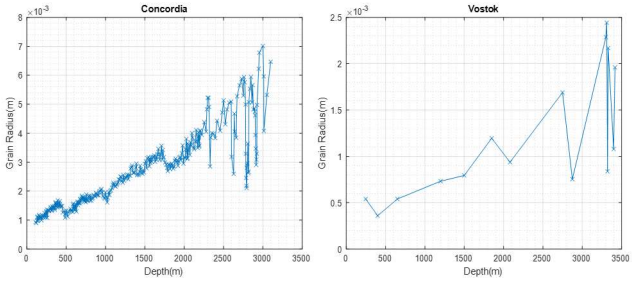

Figure 2: In-situ measurements of grain size versus depth at Concordia and Vostok stations in Antarctica.

3. RADIATION MODEL AND RETRIEVAL STUDIES

A forward electromagnetic emission model explained in [1] for the firn surface brightness temperatures were used to calculate the top of the atmosphere brightness temperatures as:

$$T_{B_{toa}}(f) = T_B(z = 0, f) * K(f) + T_{B_{atm}}(f) \quad (4)$$

where $T_B(z = 0, f)$ is the brightness temperature at the firn surface at frequency f, $K(f)$ is the atmospheric attenuation factor as a function of frequency and $T_{B_{atm}}(f)$ is the atmospheric brightness temperature at frequency f. To validate the radiation model, top of the atmospheric brightness temperatures were compared to SSMIS and AMSR2 measurements. We varied density profiles versus depth to find the best matches between simulated top of the atmosphere and satellite measured brightness temperatures over Concordia and Vostok. This can be considered a first step for the retrieval studies for the physical properties of the Antarctic firn as we observed that measured brightness temperatures over Concordia and Vostok matched simulated brightness temperatures with different density profiles.

4. DISCUSSIONS

Firn density fluctuations as discussed in section 2.1 have a considerable impact on the reflection and transmission of electromagnetic radiations among the firn layers and affect the brightness temperatures measured by the microwave radiometers. Higher density fluctuations result in more internal reflections, thereby resulting in less surface emissions and overall lower brightness temperatures. This may explain the brightness temperature differences between Vostok, and Concordia stations as seen in Figure 1 where the brightness temperatures over Concordia are higher than those over Vostok especially at intermediate and higher frequencies. Considering such differences are much smaller in vertical polarization which is less susceptible to internal reflections, we have discussed mainly horizontal polarization in this paper. Figure 3 depicts measured brightness temperatures and simulated top of the atmosphere brightness temperature best fits for all frequencies over the Concordia and Vostok stations. Changes in the measured brightness temperatures between the two locations, specifically at higher frequencies, could be simulated by varying the standard deviation ($\sigma_{density}$) of the gaussian random process which defines the density fluctuations due to internal layering.

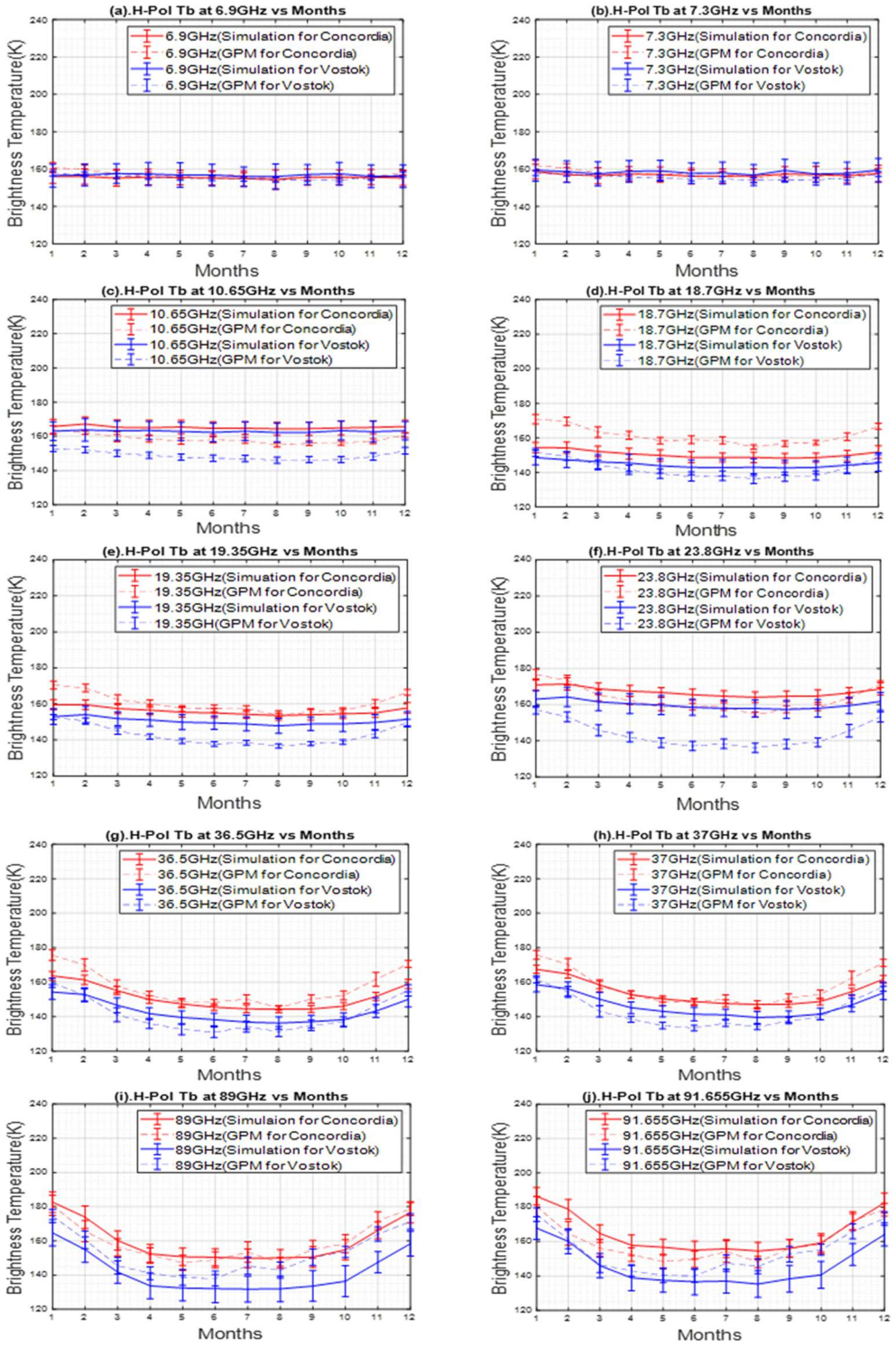

Figure 3: Comparative Analysis of calculated and measured brightness temperatures between Concordia and Vostok stations at **(a)** 6.9 GHz, **(b)** 7.3 GHz, **(c)** 10.65 GHz, **(d)** 18.7 GHz, **(e)** 19.35 GHz, **(f)** 23.8 GHz, **(g)** 36.5 GHz, (**h**) 37 GHz, (**i**) 89 GHz, and **(j)** 91.65 GHz.

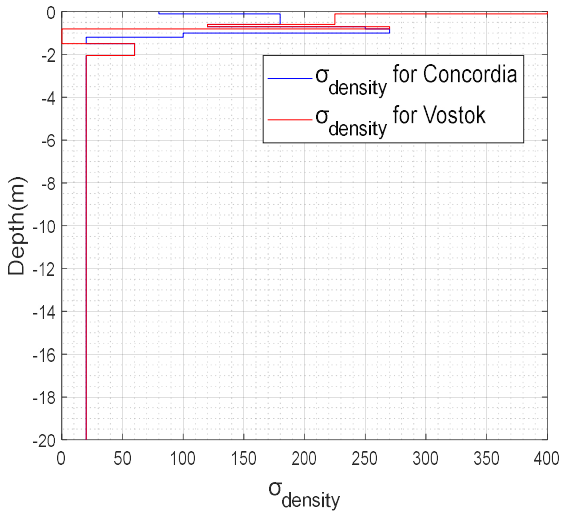

Figure 4: Variations in $\sigma_{density}$ between Concordia and Vostok stations to match calculated and measured brightness temperatures at these locations.

5.CONCLUSIONS

Assuming all other characteristics are similar around the two stations, differences in brightness temperatures could be explained with higher density fluctuations within the near-surface firn at Vostok station. A simple retrieval study for the firn density versus depth has been performed using the satellite measurements with the models for electromagnetic radiation and physical firn properties to validate this hypothesis. Figure 4 shows the retrieved density fluctuations described by the parameter $\sigma_{density}$ for both stations. As seen in the figure, $\sigma_{density}$ values are higher near the surface for the Vostok station, as expected. Higher frequencies, leading to smaller electromagnetic penetration depths, are sensitive to near-surface layers of the firn (electromagnetic penetration depth changes with frequency in ice [5]). Thus, brightness temperatures at higher frequencies over Vostok are much lower than those over Concordia due to higher density fluctuations in these layers. On the other hand, for deeper ice, which is probed at lower frequencies, there is no considerable difference in $\sigma_{density}$ between the two locations; and the brightness temperatures at such frequencies are similar.

6. ACKNOWLEDGEMENT

This study is based on the research supported by the National Science Foundation under Grant no.1844793.

The AMSR2 and SSMIS data were obtained from the NASA Goddard Space Flight Center's Precipitation Processing System (PPS) [6] and the Globe Portal System (G-Portal) of JAXA [7].

7. REFERNCES

[1] Kar, Rahul, Mustafa Aksoy, Jerusha Devadason, and Pranjal Atrey. "Potential of Global Precipitation Measurement Constellation for Characterizing the Polar Firn." *2021 IEEE International Geoscience and Remote Sensing Symposium*, Belgium, 2021, pp. 5607-5610.

[2] Jezek, K.C, Joel T. Johnson,S.Tan, L.Tsang, Mark J.Andrews, M.Brogioni, G.Macelloni, M.Durand, C.C Chen, D.J Belgiovane, and Y.Duan. "500–2000-MHz brightness temperature spectra of the northwestern greenland ice sheet." *IEEE Transactions on Geoscience and Remote Sensing* 56, no.3(2017):1485-1496.

[3] Durand, G. and J. Weiss, et al. EPICA Dome C Ice Cores Grain Radius Data. IGBP PAGES/World Data Center for Paleoclimatology Data Contribution Series # 2004-039. *NOAA/NGDC Paleoclimatology Program,* Boulder CO, USA,2004.

[4] Baker, Ian, and Rachel Obbard. "Microstructural Location and Composition of Impurities in Polar Ice Cores." *US Antarctic Program (USAP) Data Center,*2010.

[5] Aksoy, Mustafa. "Retrieval of Near-Surface Ice Sheet Properties Using the Global Precipitation Measurement (GPM) Radiometer Constellation." *2018 IEEE International Geoscience and Remote Sensing Symposium*, Valencia, 2018, pp. 5161-5164.

[6] Precipitation Processing System. Available online: https://pps.gsfc.nasa.gov/ (accessed on 18 July 2021).

[7] G-Portal, Globe Portal System. Available online: https://gportal.jaxa.jp/gpr/?lang=en (accessed on 11 July 2021).